A Multiprobe-Per-Collector Modulated Scatterer Technique for Microwave Tomography

Majid Ostadrahimi, *Member, IEEE*, Puyan Mojabi, *Member, IEEE*, Sima Noghanian, *Senior Member, IEEE*, Joe LoVetri, *Senior Member, IEEE*, and Lotfollah Shafai, *Life Fellow, IEEE*

***Abstract*—Scattering probes with collector antennas can be utilized for microwave tomography (MWT) applications based on the modulated scatterer technique. Using this technique, we previously demonstrated a novel tomography system that utilizes a single printed-wire probe in front of each collector of a multicollector MWT system. Each collector is implemented as a multilayer Vivaldi antenna. In this letter, the number of collector antennas is reduced while maintaining the number of probes. This results in a nonuniform distribution of probes with respect to the collectors and requires special calibration techniques to infer the scattered-field at the probe location. The advantages of using such a configuration for MWT are investigated. Image reconstructions for a number of targets using data collected from this system are shown and compared to results obtained from data collected using a standard MWT system that uses only the Vivaldi antennas. It is shown that the new configuration successfully extracts useful data at the locations of the probes, resulting in good tomographic constructions.**

***Index Terms*—Imaging, microwave tomography (MWT), modulated scatterer technique (MST), near-field measurement.**

I. Introduction

DURING the past few decades, there had been a significant number of publications in the area of microwave tomography (MWT), mostly addressing imaging algorithms based on nonlinear optimization techniques. A review is available in [1]. Although imaging algorithm research is of fundamental importance, there is also a need for improved experimental systems that allow the accurate measurement of a sufficient amount of electromagnetic scattering data to ensure a robust and quantitatively accurate inversion. The majority of experimental MWT measurement systems utilize co-resident antennas that measure the field directly, and thus we refer to such systems as direct measurement systems. The number of antenna elements used in these systems varies, e.g., 16 in the work reported in [2], 24 in [3] and [4], or 64 in [5]. Co-resident antenna *direct systems* are preferable to mechanical scanning systems for speed and accuracy of data acquisition. Unfortunately, the need for a large number of measurement points is in direct conflict with another important design consideration: the requirement for a minimum spatial separation between the antenna apertures so as to minimize mutual coupling and reduce modeling error in the inversion algorithms. Thus, the number of antenna elements used in such direct measurement systems is usually determined by balancing these two important design factors.

One way to increase the number of measurement points without a significant increase in mutual coupling is to use minimally perturbing near-field probes positioned remotely from "collector" antennas. Fields at the probe locations are then inferred *indirectly* using the modulated scatterer technique (MST). Various types of probes have been used in such MST-based *indirect systems*, such as dipoles [6], or even elliptical slots [7], which are modulated using a low frequency signal to infer a specific polarization. Typically, the probes are positioned relatively close to a collector antenna to capture the small changes in the field scattered by an individual probe as it is modulated in some way. This modulation produces a change in the received voltage at the collector antennas that is proportional to the field at the probe's location [8].

We have recently converted a direct MWT system based on 24 double-layered Vivaldi antennas (DLVAs) to an indirect system [9] that uses one scattering probe per DLVA collector. Having multiple collectors enables this system to achieve a full circular scanning capability at even intervals of 15°. Each DLVA collector is equipped with a novel printed wire probe that uses five p-i-n diodes for modulation. The collectors are connected to a vector network analyzer (VNA) via a 2×24 port switch network. By successively activating and deactivating each individual probe, the required MST signals are collected. However, in this system, the number of probes equals the number of collectors, each collector has its own corresponding field probe, and each probe's relative position to its collector remains unchanged making calibration straightforward to implement. Our preliminary research based on that system confirmed that a relatively flexible MST configuration is possible and indicated that major advantages might be achievable if multiple probes could be used with each collector, thus providing an increased number of field measurement positions while retaining a sparse configuration of the more bulky collector antennas.

In this letter, we show how the number of collectors can be reduced while maintaining the number of probes to be equal or greater than the collectors. Several configurations have been tested and compared with respect to their imaging performance; in these configurations, each collector interacts with 2–4 probes with various relative separations between the probes and collector. It is shown that utilizing several

Manuscript received October 06, 2011; revised November 29, 2011; accepted December 02, 2011. Date of publication December 09, 2011; date of current version December 26, 2011. This work was supported by the Natural Sciences and Engineering Research Council of Canada and the University of North Dakota.

M. Ostadrahimi, P. Mojabi, J. LoVetri, and L. Shafai are with the Department of Electrical and Computer Engineering, University of Manitoba, Winnipeg, MB R3T 5V6, Canada (e-mail: Joe_LoVetri@umanitoba.ca; shafai@ee.umanitoba.ca).

S. Noghanian is with the Department of Electrical Engineering, University of North Dakota, Grand Forks, ND 58202-7165 USA.

Color versions of one or more of the figures in this letter are available online at http://ieeexplore.ieee.org.

Digital Object Identifier 10.1109/LAWP.2011.2179110

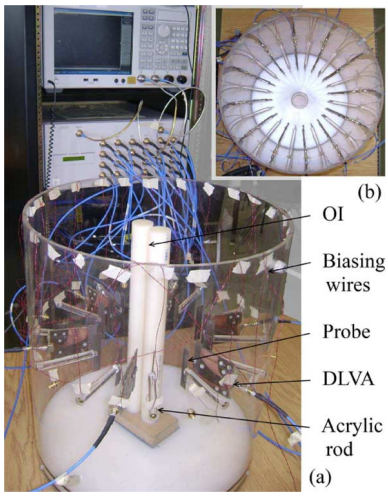

Fig. 1. Photograph of (a) six DLVA-12 probes and (b) top view of 12 DLVA, 24 probes.

probes per collector allows the acquisition of independent scattered-field data resulting in improved image reconstruction, even for probe-collector configurations where the relative distances between probes and collectors vary significantly. To evaluate the probe-based system performance, images are compared to data collected using our direct DLVA system. Four different objects of interest (OIs) are used to test these systems by reconstructing the real and imaginary parts of the OIs' dielectric profiles. The advantages of using multiple probes per collector are clearly demonstrated.

II. System Description

The description of the probe and the measurement setup is reported in detail in [9]. We use an RF switch and a VNA to capture a differential δS_{21} corresponding to "ON" and "OFF" biasings of a probe's p-i-n diodes. That is, δS_{21} is the subtraction of S_{21} for a single transmitter (Tx) and a single collector when a collector's probe is closed and opened, respectively. δS_{21} is proportional to the E_z at the probe's location. A photograph of the measurement system is shown in Fig. 1(a). While a Tx DLVA is transmitting, individual probes are successively activated while all remaining probes are kept opened ("invisible" to the field). The use of five p-i-n diodes in series causes less field perturbation by the probes, thus reducing the mutual coupling between the inactive probes [9]. In the configurations studied herein, some probes are attached directly to a DLVA, while others are held in place by acrylic rods 1.5 cm in diameter and 10.0 cm in length; see Fig. 1.

A. Near Field of a DLVA

The computed near-field E_z radiation of a single DLVA (Ansoft HFSS software) and the location of side and front probes are illustrated in Fig. 2. The field is symmetrical and directed toward the center of the chamber. Therefore, because the E_z field at the symmetrically placed left and right probes is significantly different from the probe placed directly in front of the antenna, the DLVA–probe interaction will vary.

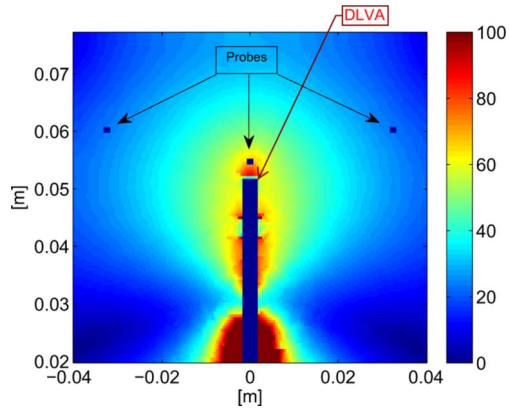

Fig. 2. $|E_z|$ near-field radiation of a single DLVA at 3.5 GHz (V/m).

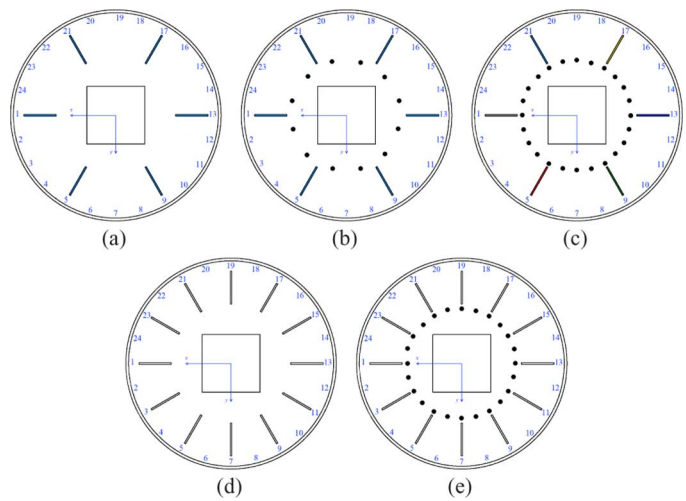

Fig. 3. Block diagram of measurements: (a) 6Tx-5Rx. (b) 6Tx-10Probe. (c) 6Tx-20Probe. (d) 12Tx-11Rx or 6Tx-11Rx. (e) 12Tx-22Probe.

TABLE I
List of Datasets. Collector is Denoted by Cx

#Ant.	#Probes	Setup	OI	Dataset
6 (6Tx-5Rx)	-	Fig. 3(a)	Fig. 4(a)	30
6 (6Tx-5Cx)	10	Fig. 3(b)	Fig. 4(a)	60
12 (12Tx-11Rx)	-	Fig. 3(d)	Fig. 4(b,c)	132
12 (12Tx-11Cx)	22	Fig. 3(e)	Fig. 4(b,c)	264
6 (6Tx-5Cx)	10	Fig. 3(b)	Fig. 4(d)	60
6 (6Tx-5Cx)	20	Fig. 3(c)	Fig. 4(d)	120

B. Measurement Systems

We report on five different measurement configurations with six or 12 Tx DLVAs, including no-probe (direct) and probe-based (indirect) systems. The receiving mode of these systems is denoted by "Rx" and "probe", respectively. The imaging tests and results corresponding to the two system types are labeled using "Rx" or "probe" and are listed in Table I.

Fig. 3(a) shows a system with six DLVAs. Data are collected using the six Tx DLVAs and five Rx DLVAs for each Tx. Note that probes are not used here. The number of data points within the acquired dataset is $6 \times 5 = 30$.

Fig. 3(b) shows a system with six DLVAs and 10 probes. Each DLVA is used as a Tx with five collector DLVAs that collect the

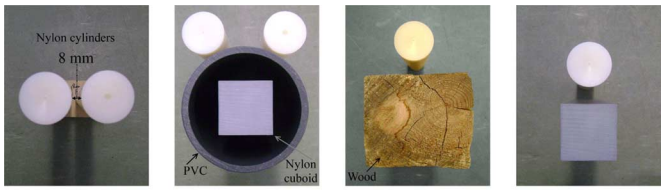

Fig. 4. Photographs of phantoms. (a) Resolution test. (b) Bear-face phantom. (c) Lossy OI test: wood-nylon rod. (d) Geometry test: nylon rod-cuboid.

TABLE II
MEASURED PERMITTIVITY AT 3.5 GHZ AND DIMENSIONS OF OIS (FIG. 4)

OI	Dimension (in cm)	Relative Permittivity
Nylon rod	$D = 3.8$	$2.64 - j0.02$
Nylon cuboid	5.0×5.0	$2.57 - j0.04$
PVC	$D_{in}, D_{out} = 10.2, 13.0$	$2.20 - j0.01$
Wood	10.0×9.5	$2.52 - j0.17$

fields from their corresponding left and right probes. In this implementation, the probes are located symmetrically with respect to their collector. The probe–collector interaction is the same for both probes, and the dataset is $6 \times 10 = 60$.

Fig. 3(c) shows a similar system with six DLVAs and 24 probes. Again, for each of the six Tx DLVAs, there are five collector DLVAs that collect the fields from four corresponding probes: right, front, left, and far left (the one to the left side of the left probe). In this implementation, the probes–collector interaction changes significantly. The dataset is $6 \times 20 = 120$.

In Fig. 3(d), the dataset size was increased by using 12 DLVAs. Here, no probes are used, and 11 Rx DLVAs collect the field for each Tx. The dataset is thus $12 \times 11 = 132$.

Fig. 3(e) illustrates a system with 12 DLVAs and 24 probes. There are 11 collectors in this system for each Tx, each of which collects the field from its left and front probes. The dataset is $12 \times 22 = 264$.

C. Objects for Imaging

The sizes of the collected datasets corresponding to the five systems are different. Thus, because more data is required for imaging more complicated OIs, a series of OIs ranging from relatively simple to more complex was chosen. Fig. 4 shows photographs of the four different OIs that were used for this study. The reconstruction was performed at 3.5 GHz. In order to validate the results, we measured the complex permittivity of each OI, $\epsilon(\mathbf{r}) = \epsilon'(\mathbf{r}) - j\epsilon''(\mathbf{r})$, using Agilent 85070E dielectric probe kit. The dimensions and measured ϵ are listed in Table II. For the wood, the reported permittivity is an average of measurements taken at its four faces.

D. Inversion Algorithm and Calibration

Multiplicative regularized Gauss–Newton inversion [10] is utilized for all reconstructions. The imaging domain S is a square (Fig. 3) that is discretized into $N \times N$ pixels, here $N = 70$. The collected scattered fields are calibrated to the scattered fields by a perfect electric conductor (PEC) reference cylinder ($D = 3.5$ in). The calibration factor for each probe–collector pair is determined as the ratio of analytical to the measured scattered field at each probe location; see [9].

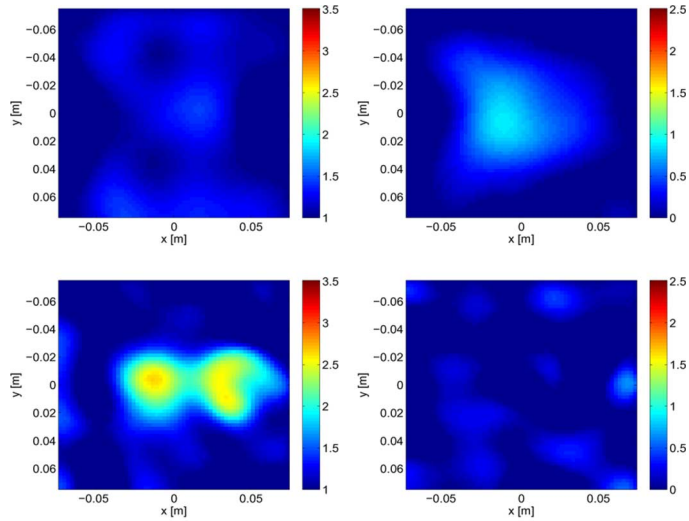

Fig. 5. Reconstructed *(left)* $\mathrm{Re}(\epsilon)$ and *(right)* $\mathrm{Im}(\epsilon)$ of 2-Nylon rods at 3.5 GHz. First row: 6Tx-5Rx. Second row: 6Tx-10Probe.

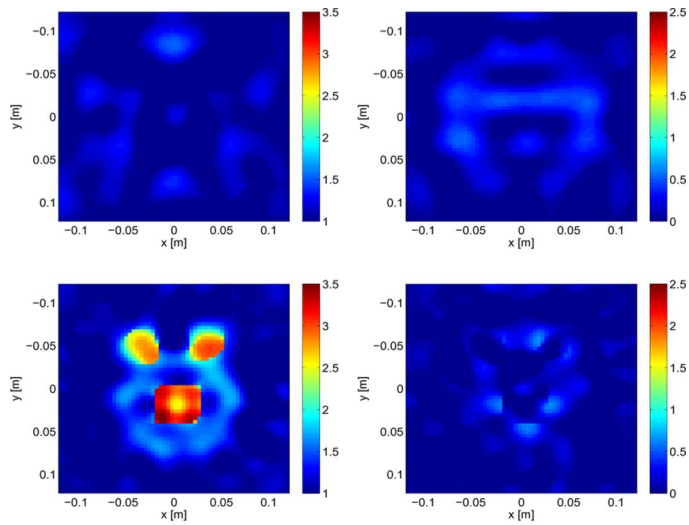

Fig. 6. Reconstructed *(left)* $\mathrm{Re}(\epsilon)$ and *(right)* $\mathrm{Im}(\epsilon)$ of the bear-face phantom. First row: 12Tx-11Rx. Second row: 12Tx-22Probe.

III. IMAGING RESULTS

In this section, the reconstructed images of different OIs are presented. For the first test, imaging results are presented for the six-DLVA system using either five Rx DLVAs [Fig. 3(a)] or 10 symmetrical probes on the left and right of each collector [Fig. 3(b)]. Due to the small amount of information possible using these systems, only the simplest resolution test OI was used [Fig. 4(a)]. The resulting reconstructions are shown in Fig. 5 (the reconstructions for the other OIs were poor because of the small amount of data collected).

The second results are for the 12-DLVA system using either 11 Rx [Fig. 3(d)] or 22 asymmetrical probes on the left and front of each collector [Fig. 3(e)]. The dataset is large enough for imaging a more complex OIs: the bear-face phantom [Fig. 4(b)] and the wood-nylon lossy object [Fig. 4(c)]. The reconstructed images are shown in Figs. 6 and 7.

For the third test, the performance of increasing the number of probes in an indirect system is investigated, where now the relative probe–collector distances vary significantly. Only six

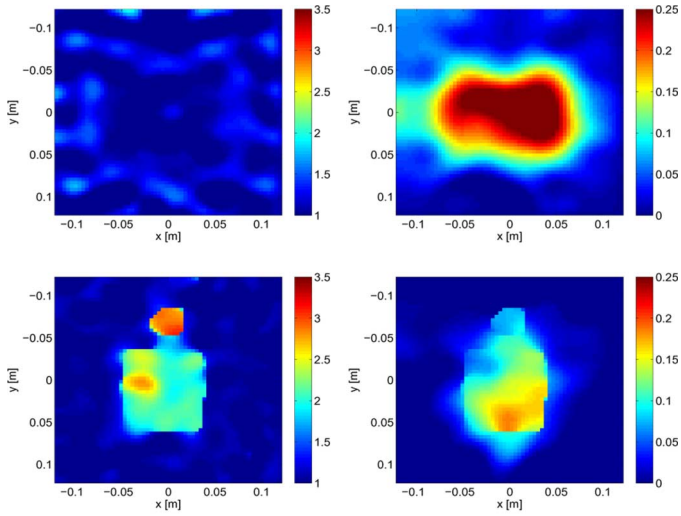

Fig. 7. Reconstructed *(left)* $\mathrm{Re}(\epsilon)$ and *(right)* $\mathrm{Im}(\epsilon)$ of the wood-nylon phantom. First row: 12Tx-11Rx. Second row: 12Tx-22Probe.

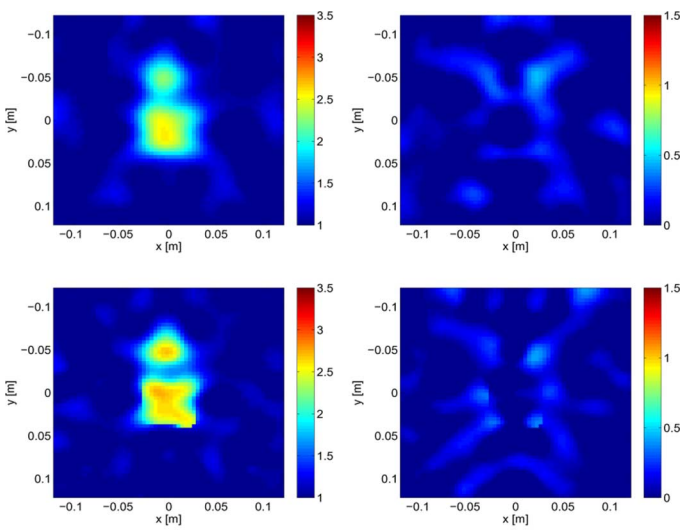

Fig. 8. Reconstructed *(left)* $\mathrm{Re}(\epsilon)$ and *(right)* $\mathrm{Im}(\epsilon)$ of the nylon rod-cuboid phantom. First row: 6Tx-10Probe. Second row: 6Tx-20Probe.

DLVAs are used with either 10 or 20 probes (see Table I). The imaged OI is the geometry test OI of Fig. 4(d), and its reconstructed images are shown in Fig. 8.

IV. Discussion

The results of Fig. 5 clearly show that image reconstruction with the 6Tx-5Rx system is not possible, but using probes in the 6Tx-10Probe system to double the amount of collected information produces reasonable results. Note that both systems use six DLVAs, but the probes allow one to infer the scattered field at more locations per Tx DLVA. Similar results are obtained for the reconstruction of a more complicated phantom, the bear-face, shown in Fig. 6, where now only 12 antennas are used for measurement. Image reconstruction fails using the 12Tx-11Rx system, while the 12Tx-22Probe system clearly reconstructs the bear-face OI. The results for the wood-nylon OI of Fig. 7 confirm that the introduction of extra probes allows independent data useful for image reconstruction.

The rod-cuboid geometry test imaging results shown in Fig. 8 use six Tx and five collector antennas, with the number of probes changing from 10 to 20. For this case, the use of 20 probes with only five collectors requires the use of probes whose angular separation from the collector is 30°, and their relative distance from their collector is significantly different from the ones that are in front of the collector, making proper calibration essential. When the full set of 20 probes is used, accuracy of the reconstruction is better compared to the 6Tx-10Probe system, which confirms that even adding probes at a large distance from the collector can add useful data that improves the image reconstruction.

V. Conclusion

One disadvantage of direct-measurement MWT systems is the limitation of the number of possible measurement locations. The flexible MST-based indirect system reported here shows that the number of probing sites can be increased while maintaining a small number of co-resident collector antennas that also maintain a sufficiently low mutual coupling. It was shown that the significant difference in probe–collector interaction in these nonuniform multiprobe-per-collector systems can be compensated. Imaging results show that a direct system with a small number of co-resident antennas is not able to reconstruct some OIs, whereas an indirect system with the same number of antennas used as collectors but with a greater number of probes increases the amount of collected data and successfully reconstructs the same OI. This confirms that the additional probe data generate independent information that is useful for image reconstruction. In addition, increasing the number of probing locations does not add substantially to the costs of implementing such systems.

References

[1] M. Pastorino, *Microwave Imaging*. Hoboken, NJ: Wiley, 2010.
[2] P. Meaney, M. Fanning, D. Li, S. Poplack, and K. Paulsen, "A clinical prototype for active microwave imaging of the breast," *IEEE Trans. Microw. Theory Tech.*, vol. 48, no. 11, pp. 1841–1853, Nov. 2000.
[3] S. Semenov, J. Kellam, Y. Sizov, A. Nazarov, T. Williams, B. Nair, A. Pavlovsky, V. Posukh, and M. Quinn, "Microwave tomography of extremities: 1. Dedicated 2D system and physiological signatures," *Phys. Med. Biol.*, vol. 56, pp. 2005–2005, 2011.
[4] C. Gilmore, P. Mojabi, A. Zakaria, M. Ostadrahimi, C. Kaye, S. Noghanian, L. Shafai, S. Pistorius, and J. LoVetri, "A wideband microwave tomography system with a novel frequency selection procedure," *IEEE Trans. Biomed. Eng.*, vol. 57, no. 4, pp. 894–904, Apr. 2010.
[5] N. Joachimowicz, J. Mallorqui, J. Bolomey, and A. Broquets, "Convergence and stability assessment of Newton–Kantorovich reconstruction algorithms for microwave tomography," *IEEE Trans. Med. Imag.*, vol. 17, no. 4, pp. 562–570, Aug. 1998.
[6] T. Henriksson, N. Joachimowicz, C. Conessa, and J. Bolomey, "Quantitative microwave imaging for breast cancer detection using a planar 2.45 GHz system," *IEEE Trans. Instrum. Meas.*, vol. 59, no. 10, pp. 2691–2699, Oct. 2010.
[7] M. Aboukhousa, M. Ghasr, S. Kharkovsky, D. Pommerenke, and R. Zoughi, "Modulated elliptical slot antenna for electric field mapping and microwave imaging," *IEEE Trans. Antennas Propag.*, vol. 59, no. 3, pp. 733–741, Mar. 2011.
[8] J. Bolomey and F. Gardiol, *Engineering Applications of the Modulated Scatterer Technique*. Norwood, MA: Artech House, 2001.
[9] M. Ostadrahimi, P. Mojabi, S. Noghanian, L. Shafai, S. Pistorius, and J. LoVetri, "A novel microwave tomography system based on the scattering probe technique," *IEEE Trans. Instrum. Meas.*, 2011, to be published.
[10] P. Mojabi and J. LoVetri, "Microwave biomedical imaging using the multiplicative regularized Gauss–Newton inversion," *IEEE Antennas Wireless Propag. Lett.*, vol. 8, pp. 645–648, 2009.